# Dynamically-figured mirror system for high-energy nanofocusing at the ESRF

**Article** *in* Proceedings of SPIE - The International Society for Optical Engineering · September 2011

DOI: 10.1117/12.894735



**9 authors**, including:

Yves Dabin
European Synchrotron Radiation Facility
**27** PUBLICATIONS **342** CITATIONS
SEE PROFILE

Heikki Suhonen
University of Helsinki
**85** PUBLICATIONS **1,253** CITATIONS
SEE PROFILE

Rémi Tucoulou
European Synchrotron Radiation Facility
**155** PUBLICATIONS **1,940** CITATIONS
SEE PROFILE

Amparo Vivo
European Synchrotron Radiation Facility
**48** PUBLICATIONS **446** CITATIONS
SEE PROFILE

# Dynamically-figured mirror system for high-energy nanofocusing at the ESRF

R. Barrett, R. Baker, P. Cloetens, Y. Dabin, C. Morawe, H. Suhonen, R. Tucoulou, A. Vivo, L. Zhang
European Synchrotron Radiation Facility, BP220, 38043 Grenoble Cedex 09, France

## ABSTRACT

The design, manufacture and characterization of a Kirkpatrick-Baez (KB) configuration mirror system for high-throughput nanofocusing down to 50 nm beam sizes are described. To maximize the system aperture whilst retaining energy tunability, multilayer coated optics are used in conjunction with 2 dynamically figured mirror benders. This approach, which has been developed at the ESRF for many years, allows the focusing performance to be optimized when operating the system in the 13–25 keV photon energy range. Developments in the key technologies necessary for the production of mirror bending systems with dynamic figuring behavior close to the diffraction limit requirements are discussed. These include system optimization via finite element analysis (FEA) modeling of the mechanical behavior of the bender-mirror combination, manufacturing techniques for precisely-shaped multilayer substrates, multilayer deposition with steep lateral gradients and the stitching metrology techniques developed for the characterization and figure optimization of strongly aspherical surfaces. The mirror benders have been integrated into a compact and stable assembly designed for routine beamline operation and results of the initial performance of the system at the ESRF ID22NI endstation are presented demonstrating routine focusing of 17 keV X-rays to sub-60 nm resolution.

**Keywords:** x-ray optics, x-ray multilayers, Kirkpatrick-Baez mirrors

## 1. INTRODUCTION

Reflective optics are often used as the final focusing element for X-ray micro- and nano-probe beamlines at synchrotron light sources. Due to the manufacturing difficulties of producing the ideal ellipsoidal surface figure necessary for 2-d 'point-to-point' imaging of a real source by a single optical element, it is common to use two discrete mutually orthogonal reflective surfaces arranged in either the 'Kirkpatrick-Baez' (KB) configuration [1] or the Montel scheme [2]. In this case, the optimal surface figure of each of the two components becomes an elliptical cylinder, thus reducing considerably the complexity of manufacture. One method of developing the necessary elliptical surfaces is to use deterministic manufacturing processes coupled with appropriate metrology techniques to produce the two statically-figured mirror elements. Systems based upon optics of this type assembled into the KB [3] or Montel [4] configuration have both demonstrated two-dimensional focusing of hard X-rays (15-30 keV) to the 200 nm (fwhm) scale and below. For line-focusing, a statically figured mirror has demonstrated focusing of 20 keV X-rays to 7 nm (fwhm) [5].

An alternative approach explored by several groups is to develop the required surface figure by controlled mechanical bending of a (usually) flat substrate [6-8] via two moments applied to the ends of the mirror. With such methods, the mirror substrate becomes easier to manufacture to high quality but at the expense of a significantly more complex optomechanical implementation. Generally the substrate bending can be remotely actuated and thus the optical surface figure can be flexibly adjusted to optimise the focusing conditions (e.g. working distance, mirror grazing angle) depending on the experimental requirements. At the ESRF, dynamically-figured mirror systems based upon flexural hinge-type bending mechanisms [9] have been developed for over ten years. Generic bender formats [10] have been designed allowing the implementation of KB systems with 300 mm, 170 mm and 92 mm long mirrors. These bender technologies have been installed at 20 ESRF beamlines. In a demonstration experiment, the ESRF bender design was shown to be capable of diffraction limited line focusing to 41 nm fwhm [11]. In a more standard configuration for routine operation in beamline 'user-mode', 2-dimensional focusing to a spot size of 76 nm x 84 nm has been previously reported at 17 keV at the ESRF ID22 undulator beamline.

In many practical applications for hard X-ray focusing it is advantageous to deposit reflective multilayer (ML) coatings on the figured optical surfaces [11]. Over one third of the currently deployed bender systems at the ESRF incorporate

Advances in X-Ray/EUV Optics and Components VI, edited by Christian Morawe, Ali M. Khounsary, Shunji Goto,
Proc. of SPIE Vol. 8139, 813904 · © 2011 SPIE · CCC code: 0277-786X/11/$18
doi: 10.1117/12.894735

ML coated optics. This permits the use of higher grazing angles than is possible with total-reflection coatings and reduces the necessary mirror length for a given aperture size. The use of such coatings is also imperative for applications aiming for highest resolutions since the critical angle of total-reflection coatings places a fundamental limit on the maximum attainable numerical aperture (NA). For the KB configuration, this limits the smallest practical focused beam size to around 20 nm [12].

As part of the new ID22NI beamline endstation, specifically designed for nanoprobe and nanoimaging applications, the requirement for a compact optical system capable of providing a high flux focused monochromatic X-ray beam with dimensions of 60 x 60 $nm^2$ over a photon energy range of 13 — 25 keV, provided an opportunity to explore some of the practical limits of the ESRF technologies aiming for routine operation of dynamically figured mirror KB systems for nanofocusing applications. In the following, we describe the system design, associated technological developments and performance of the system which is now in routine operation at ID22NI.

## 2. ID22NI KB SYSTEM

### 2.1 System optical design

The ID22 beamline uses an undulator source located on a high-β section of the ESRF storage ring. For operation with the low vertical emittance mode of the ESRF, the effective fwhm (horizontal x vertical) source sizes are 970 x 12 $\mu m^2$. A variable gap, 19 mm-period undulator allows tunability of the operating energy in the 13 — 30 keV range with an intrinsic energy band width of the corresponding emission peak of ~1.7%. The monochromaticity requirements for the ID22NI endstation are modest: an energy band-pass of several percent is sufficient for the targeted experimental applications (X-ray fluorescence microscopy, projection microscopy and scanning coherent diffraction imaging). More important is to maximize the focused flux; Consequently, optics upstream of the KB system are limited to a single horizontally deflecting plane total-reflection mirror for harmonic rejection. The focusing mirror system uses wide band-pass multilayer coatings to accept the full energy band width of the undulator emission peak whilst maximizing the aperture. In operation, the absorbed power upon the upstream (vertically deflecting) KB mirror is less than 1 W and no active cooling of the system is required. The horizontal focusing optic cannot accept the full source emittance whilst delivering the required sub-60 nm focal spot size. Achieving the necessary spot-size necessitates the introduction of a narrow slit which limits the effective source size; At ID22, this approach had been tested with a previous KB system using a slit placed 27 m from the source and typically adjusted to 10 μm wide. The chosen optical configuration means that the vertical X-ray beam emittance is essentially unmodified upstream of the KB system. Consideration of the required spot size, the necessary experimental constraints to allow space for sample environment and manipulation led to the choice of the optical parameters for the KB system given in

Table 1. Due to the use of multilayer coatings and the need to operate at variable energies, the grazing angle must be adjusted for each energy and hence the elliptical figure of the mirrors must be modified at each angular setting. This is one of the primary motivations for using dynamic figuring technologies. The basic system consists of two orthogonal ESRF designed mirror bending mechanisms. By placing the horizontal mechanism downstream the intrinsic ellipticity of the photon source is reduced (the aim in most experiments being to use a circular spot focus).

### 2.2 Substrate profile optimization

The application of two independent bending moments to the ends of the mirror substrate as in the ESRF bender design develops a linear variation of the moment along the mirror length. For the aspherical (elliptical) profile required, the radius of curvature R(x) of the bent substrate varies strongly with position x along the mirror length. The required variation over the useful mirror length for the ID22NI system is given in

Table 1. Using mechanical beam theory approximation, the local curvature, 1/ R(x), can be calculated by:

$$\frac{1}{R(x)} = \frac{d^2u}{dx^2} = \frac{M(x)}{EI(x)} \text{ with } I(x) = \frac{W(x)t^3(x)}{12} \quad (1)$$

where $u$ is the vertical displacement of the mirror, $x$ the mirror coordinate, $M(x)$ the local bending moments. $E$ and $I(x)$ respectively elastic modulus and local moment of inertia of the mirror. $W(x)$ and $t(x)$ are the local width and thickness of the substrate respectively.

| | Vertical Focusing Mirror (VFM) | Horizontal Focusing Mirror (HFM) |
|---|---|---|
| Useful mirror length [mm] | 70 | 40 |
| Entrance arm, $p$ [m] | 63 | 36 |
| Exit arm, $q$ [m] | 0.18 | 0.083 |
| Radius of curvature, $R(x)$, range along useful mirror length (at 8 mrad) [m] | 58 — 32 | 29 — 14 |
| Target rms slope error [μrad] | <0.15 | <0.1 |
| Grazing angle, $\theta$ [mrad] | 5.5 (25 keV) – 10.7 (13 keV) | |

Table 1: Optical design configuration for the ID22NI KB system

For a rectangular prism, $I(x)$ is constant and allows a 3rd order polynomial approximation to the ideal elliptical cylinder surface figure. For the mirror lengths and bending radius required for the ID22NI system the figure/slope errors for this substrate geometry would be incompatible with the target performance. To overcome this limitation, a commonly applied approach at the ESRF is to use a trapezoidal profile for the mirrors i.e. a linear variation in the substrate width, $W(x)$, along the mirror. This allows correction of higher order terms in the elliptical figure expansion. For improved correction of the figure errors it is necessary to use more complex width profiles (quadratic and beyond). For manufacturing simplicity the substrate thickness, $t(x)$, remains constant along the mirror length. This analytical approach is valid assuming that pure bending moments are applied to the mirror and that the assumptions of the underlying beam theory are valid. Finite element analysis (FEA) offers a method to include the influence of the mechanical bender and its constraints. In particular, the (i) bender stiffness, (ii) anticlastic effects, (iii) geometrical nonlinear effects all influence the bent substrate figure and will modify the optimum shape profile. Use of an iterative FEA modeling procedure [13], allows optimization of the mirror width profile for a particular optical configuration ($p$, $q$ and $\theta$). The initial mirror profile for the process used the optimum trapezoidal profile calculated using the analytical approximation. For the ID22NI KB system, the optimization process was performed for the mirror grazing angles of 8 mrad (corresponding to the operating conditions for focusing at 17 keV). The assembly of the Si mirror substrate and Invar flexural bender used for the FEA modeling is shown in

Figure 1. Evolution of the HFM profile between successive iterations is shown in Figure 2.

The FEA indicated that rms. slope errors of 0.13 μrad and 0.08 μrad should be attainable for the HFM and VFM respectively for operation at 17 keV (see Table 2). Using the optimized width profiles for 8 mrad as input to the FEA, it was also possible to calculate the expected slope errors over the full operating range of incidence angles. These calculations show that slope errors for higher energy operation should be somewhat reduced, whilst the highly aspheric figure required for operation at 10.7 mrad degrade the surface quality.

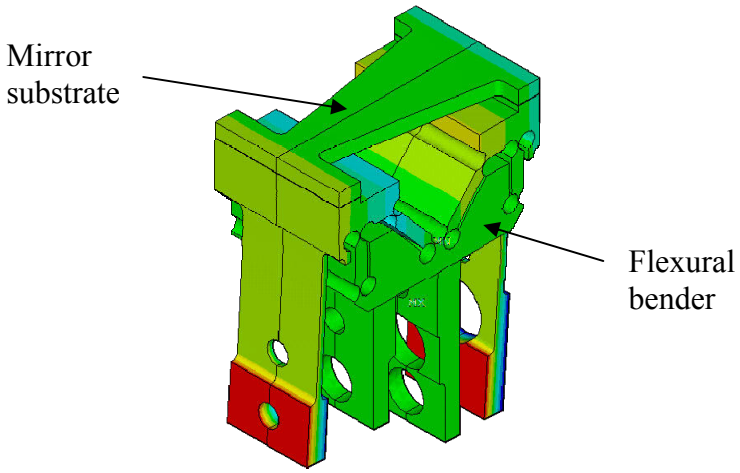


Figure 1: FEA model of the HFM mirror substrate and flexural bender assembly

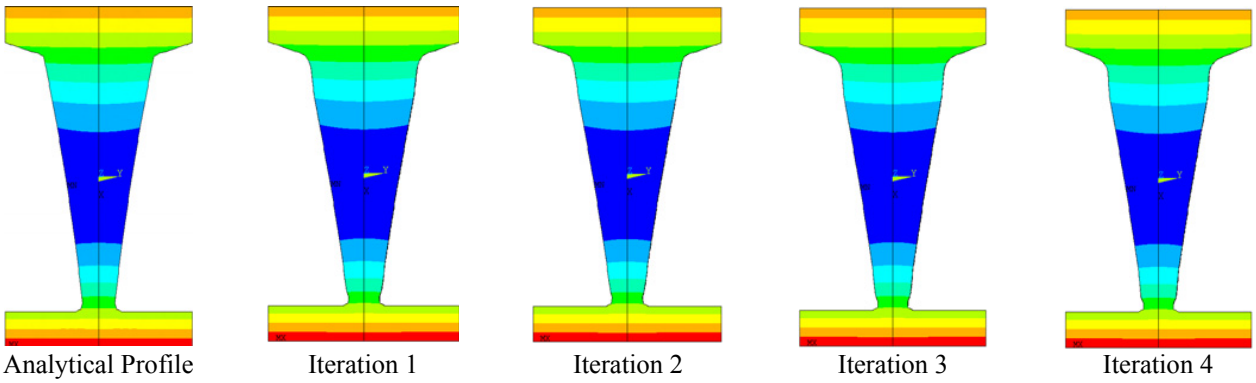


Figure 2 Schematic top view of the bent HFM mirror substrate showing evolution of the width profile at successive iterations of the FEA modeling. Colors indicate the displacement of the mirror surface normal to the originally flat substrate.

| Glancing Angle [mrad] | Energy [keV] | rms slope errors [µrad] | |
|---|---|---|---|
| | | VFM (over 70 mm) | HFM (over 40mm) |
| 5.6 | 25 | 0.06 | 0.11 |
| 8 | 17 | 0.08 | 0.13 |
| 10.7 | 13 | 0.12 | 0.17 |

Table 2: Calculated slope errors derived from FEA calculations. The mirror width profile was optimized for operation at 8 mrad.

### 2.3 Substrate manufacture

The optical quality of the substrates for the KB system influences the system performance since any residual figure errors after subtraction of a third order polynomial fit cannot be corrected by the mirror bending mechanisms. Single crystal silicon was chosen as the mirror substrate as processes for producing highly flat surfaces are well established and can be combined with the sub-Å rms surface finish which is required for high quality multilayer deposition. Bending an

initially flat substrate to a concave reflecting surface as required for the KB system develops tensile stresses at the substrate rear surface, $\sigma_{max}(x)$, which are inversely proportional to the local bending radius according to:

$$\sigma_{\max}(x) = \frac{6M(x)}{W(x)t^2(x)} = \frac{Et(x)}{2R(x)} \quad (2)$$

For the HFM, the curvature radius of 8 m at the downstream end in the low energy configuration is particularly short and the risk of substrate fracture is significant. There is a strong incentive to minimize the substrate thickness to reduce stresses but this is tempered by the difficulty of polishing thin substrates to achieve slope errors ~ 0.1 µrad rms. Thicknesses of 5 mm for the HFM and 6 mm for the VFM were chosen as an acceptable compromise but nevertheless lead to an elevated peak tensile stress for the horizontal deflecting mirror of ~ 50 MPa. Under tensile loading at room temperature, Si displays negligible plastic deformation. Consequently its ability to withstand these elevated stress levels can be predicted in terms of the fracture toughness, $K_c$, and flaws (cracks, indents...) within the tensile region (e.g.[14]). Considering Mode I loading of a sharp surface crack of given dimensions, $c$, the threshold stress, $\sigma_f$, for crack propagation (i.e. failure of the substrate) is given by:

$$\sigma_f = \frac{K_{Ic}}{\sqrt{2c\pi}} \quad (3)$$

where $K_{Ic}$ is the corresponding fracture toughness. Both the elastic properties [13] and fracture toughness [15] of Si are anisotropic. It is therefore judicious to choose a crystalline orientation of the substrate such that the ratio, $K_{Ic}/E$, is maximized. For the ID22NI KB system the substrates were oriented such that the reflecting faces were parallel to {110} with the <001> axis aligned along the mirror. Following equations 2 and 3, use of a maximum acceptable surface flaw size on the rear surface of the mirror of 50 µm should be sufficient to provide a safety factor of 2 and can be achieved by careful substrate processing. The FEA calculations indicated that a precision on the width profile, $w(x)$, of 20 µm is sufficient to ensure that any associated degradation of the slope error is <0.1 µrad rms. The profiled substrate blanks were machined from highly doped single crystal silicon using wire electrical discharge machining (WEDM) which gave a width precision for $w(x)$ of < 2 µm prior to polishing. The blanks were polished by a commercial supplier to give rms slope errors (after subtraction of the best fitting elliptical profile) over the clear apertures, measured by the ESRF Long Trace Profiler (LTP) [16] of 0.13 µrad and 0.09 µrad, for the HFM and VFM respectively. The average substrate roughness measured by 2-d microinterferometry was <1 Å rms over spatial sampling periods from 2.5 mm to 0.5 µm. The polished substrates are shown in Figure 3.

### 2.4 Multilayer deposition

Due to the short bending radii of the mirrors, the X-ray beam grazing angle varies rapidly along the mirror length: As an example, for a nominal angle of 8 mrad at the HFM mirror centre the grazing angle ranges from 7.0 to 9.4 mrad along the useful aperture. As a consequence, the multilayer deposition must provide an extremely steep lateral d-spacing gradient, for the more demanding HFM case the necessary gradient is 30% over the 40 mm long useful aperture The laterally-graded coatings were produced by dynamic magnetron sputter deposition onto the superpolished Si substrates in the ESRF Multilayer Lab [17]. The coatings on each mirror consist of 25 $W/B_4C$ bilayers ($\Gamma$= 0.5) giving a typical energetic band pass of the multilayers of ~8.5% and can diffract the full band-width of the undulator peak with a single bounce peak reflectivity at 17 keV of >70%. Figure 4 shows the d-spacing gradients of the 2 laterally graded coatings (q = 180 mm and q = 83 mm). Residual thickness errors are far below 1% (PV) and therefore negligible compared with the ML peak width. The experimental data was obtained from x-ray reflectivity scans measured at 8 keV.

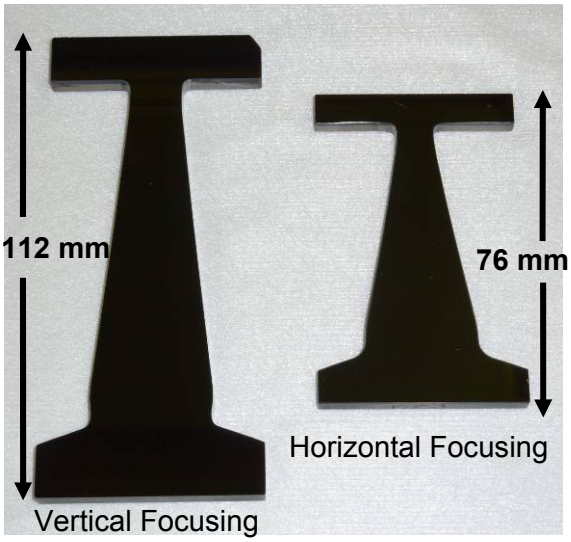


Figure 3: Polished Si substrates for ID22NI KB system

### 2.5 Mirror Bender design

The dynamical mirror figuring mechanisms are an extension of the generic flexural bender systems which are widely deployed at the ESRF. The design modifications for the ID22NI KB system aimed at producing an extremely compact, precise, stable and reliable focusing device. For nanofocusing mirror systems previous experience at the ESRF showed that thermal drifts are the primary cause of focus degradation. To minimize such effects the entire flexural bender bodies are WEDM machined from single pre-ground Invar blocks. A specific two-stage heat treatment is used to achieve optimal thermal and dimensional stability. The bending lever arms are designed to deform elastically during application of the mirror bending force in order to improve the adjustment sensitivity for mirror figuring. The integration of incremental encoders is designed to permit rapid readjustment of the mirror figure to pre-recorded values and, by improvement of the repeatability of the piezomotor actuators, speeds the convergence of the iterative figuring optimization process. As the final stage of the bender mechanism assembly the polished coated substrates are adhesively bonded to the benders to avoid any mirror distortion (in particular surface 'twist') which can be engendered by mechanical clamping. The HFM bender assembly is shown in Figure 5.

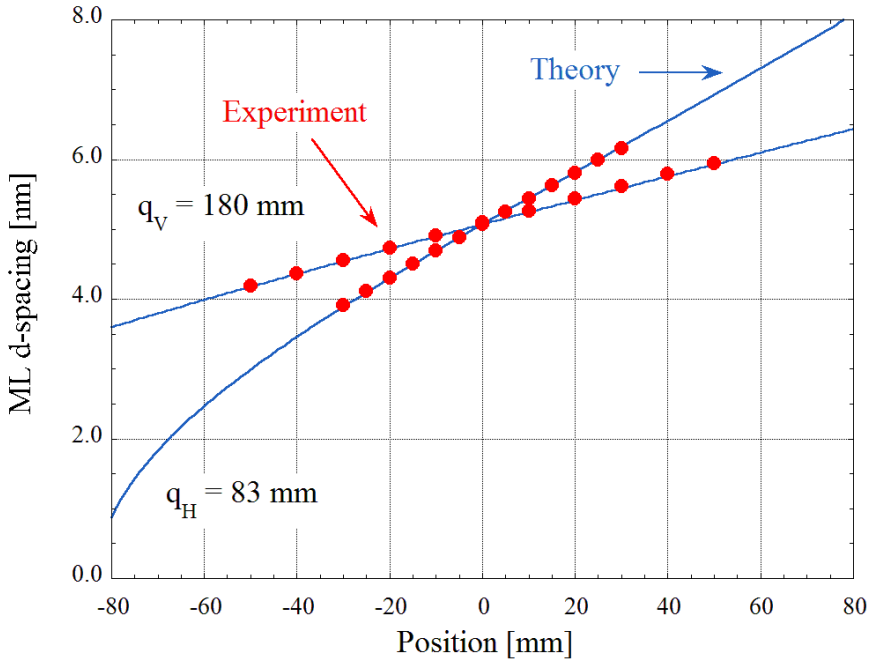


Figure 4: Theoretical target and experimentally determined multilayer d-spacing gradients for the HFM and VFM substrates

### 2.6 Optical Metrology

The performance of the flexural bender assemblies was evaluated prior to integration into the KB system using the ESRF LTP. For ultimate measurement accuracy, 'retrace' errors should be minimized. Practically this means that the angular aperture of the instrument used during measurement should be restricted as far as possible. For metrology of short radii optics, this is achieved by measuring a succession of sub-aperture profiles, tilting the optic between measurements. Results are then 'stitched' to obtain the complete mirror shape profile. Optimization of the mirror elliptical figures was performed by initial measurement of the interaction matrices [18] for each bender which allows convergence to the desired elliptical profile in typically three or four iterations (from an initial arbitrary figure). Figure 6 shows the slope and figure errors relative to the best fitting ellipse for the VFM and HFM following optimization of the mirror bending to the nominal conditions corresponding to operation at 17 keV. The figure (shape) errors are derived from numerical integration of the slope error measurements. The numerical values for adjustment at 17 and 25 keV are presented in Table 3.

| Glancing Angle [mrad] | Energy [keV] | measured rms slope errors [µrad] | | rms figure/shape errors [nm] | |
|---|---|---|---|---|---|
| | | VFM (over 70 mm) | HFM (over 40mm) | VFM (over 70 mm) | HFM (over 40mm) |
| 5.6 | 25 | 0.06 | 0.11 | 0.16 | 0.16 |
| 8 | 17 | 0.09 | 0.15 | 0.32 | 0.38 |

Table 3: Minimum slope and corresponding shape errors for each of the bender assemblies from LTP measurements following figure optimization for two of the foreseen operating energies.

The measured slope error values are very close to the optimal theoretical values given in Table 2. It is interesting to note that for both mirror assemblies the measured slope errors are better than those measured of the polished substrate prior to bonding. Currently the origin of this discrepancy remains unclear.

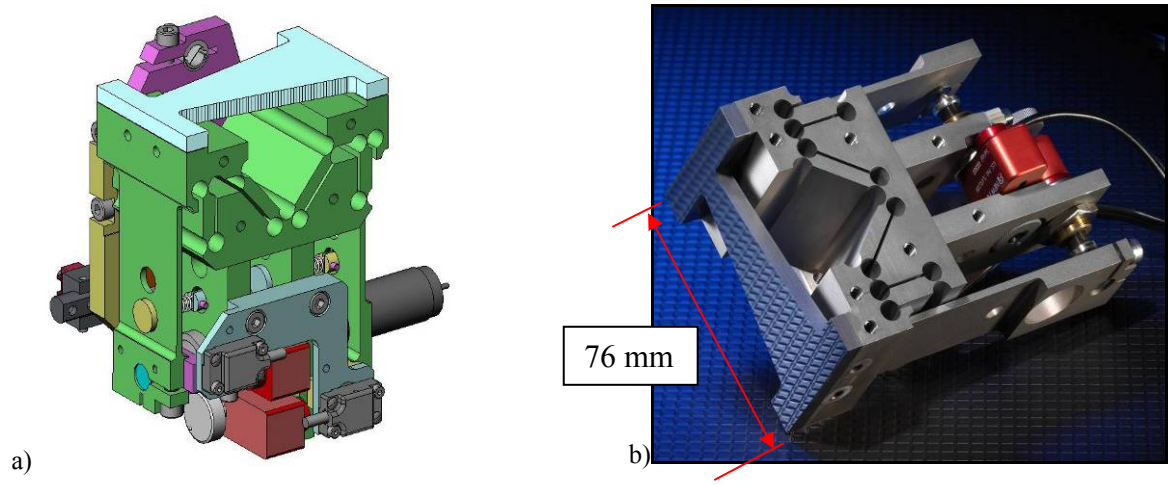


Figure 5: a) schematic design of the HFM mirror bender. b) the final assembly prior to integration in the KB system.

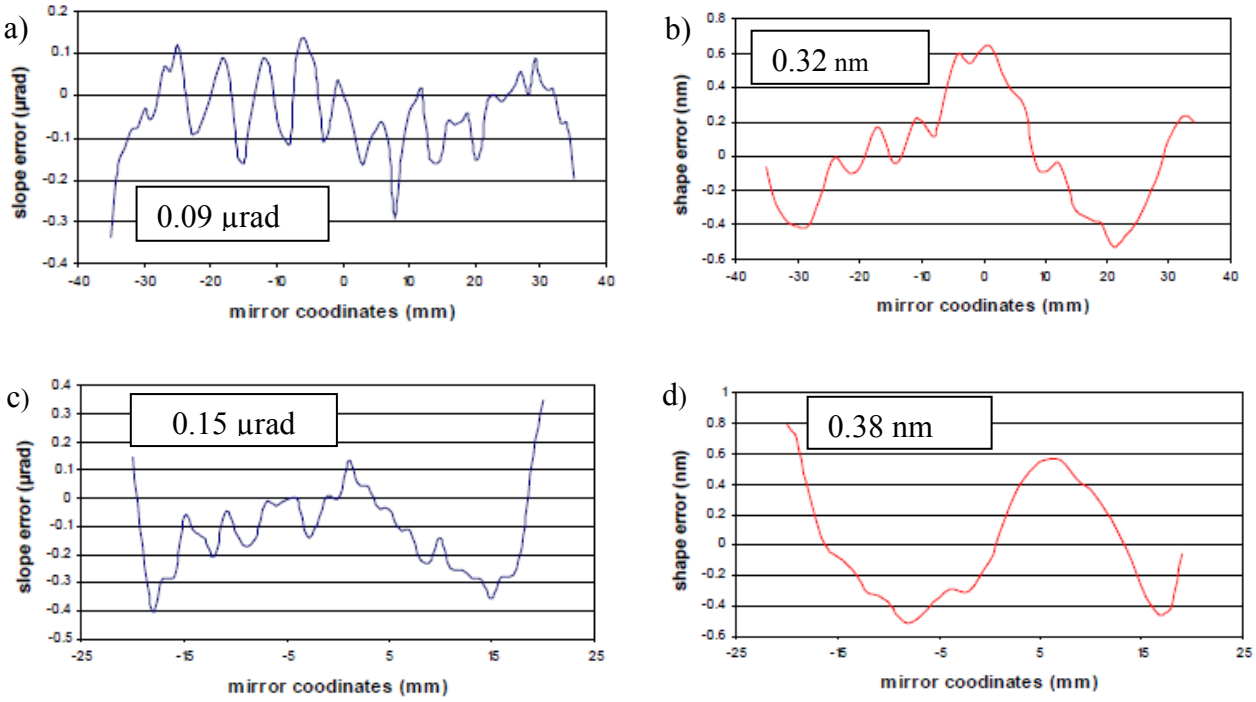


Figure 6: Measured slope and figure errors for the VFM (a and b) and the HFM (c and d) with the mirror bending optimized for operation at 17 keV (8 mrad)

### 2.7 KB system design

The bender assemblies are integrated into a KB configuration based upon a dedicated granite support. The KB system (Figure 7) provides the necessary motorized movements (the two incidence angle adjustments), manual adjustment for the mirror orthogonality and incorporates precise slits for mirror alignment and entrance aperture definition. The number of motorized displacements in the system has been deliberately reduced to the strict minimum in favor of maximum mechanical stability. As for the benders, for optimal thermal stability many of the parts are manufactured from Invar. The entire system is housed in a close-fitting environmental enclosure which improves local temperature stability and, in operation, allows continual flushing of the entire system with clean nitrogen gas to limit both particulate and volatile

organic contamination. A free working distance of 35 mm is available between the end of the enclosure and the focus position.

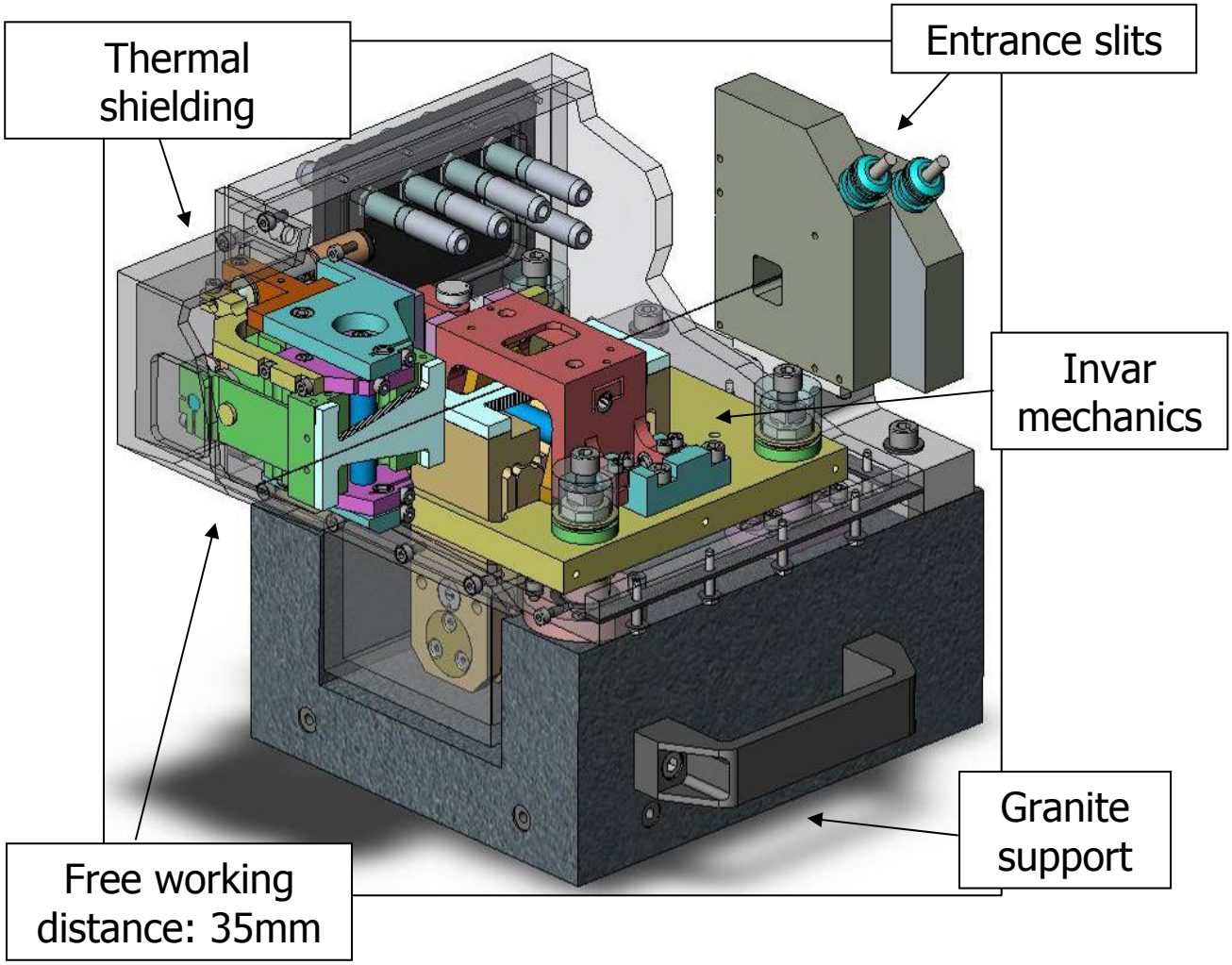


Figure 7: Schematic of ID22NI KB system

## 3. X-RAY PERFORMANCE

The KB system was installed at the ID22 beamline in August 2010. Following pre-alignment to centre the mirror apertures in the X-ray beam, the entrance slits are adjusted to around 10µm gap. This incoherent X-ray pencil beam can then be scanned to define the local illuminated footprint on the mirror surface and, in conjunction with a 2-d CCD based detector at the focal plane, provides a measurement of the local mirror slope [18]. As for the LTP measurements, the in-situ X-ray metrology measurements can be used to construct the interaction matrix and thus converge rapidly to the desired surface figure. Automated routines allow the mirror bending to be optimized in typically 1 hour from an unknown starting point. The entrance slits are then opened to define the accepted aperture of the KB system in normal operation.

Figure 8:shows resolution scans acquired by X-ray fluorescence detection of a gold knife-edge sample moved through the 17 keV focused beam to measure the horizontal and vertical spot sizes. Differentiation of these profiles yields a gaussian beam size of 59 x 43 $nm^2$ (H x V). The focused beam intensity was measured to be $10^{12}$ ph/s corresponding to a flux intensity of 1.5 $10^8$ ph/s/$nm^2$. The small intense X-ray focus provided by the KB system is well suited for use as a

source in projection phase-contrast microscopy experiments e.g. [19]. Figure 9 a and b show quantitative measurements of the X-ray phase shift at 17 keV in a gold Siemens star resolution-test structure. The 30 µm diameter 180 nm high gold structure is deposited on a 100–120 nm-thick $Si_3N_4$ membrane and has a finest feature size of 50 nm (Calibration pattern X50–30–2m, X-radia Inc., California). Transmission images of the structure are taken by placing it downstream of the focal spot at four different distances from the focus and recording an image of the transmitted intensity further down stream. Phase images are then derived using holographic reconstruction [20]. The minimum spatial resolution in these reconstructions is fundamentally limited by the size of the source i.e. the KB focus size. The reconstructions show that the innermost 50 nm structures are resolved. Figure 9c is an image of the same structure displaying the intensity variations in the Au L fluorescence emission as the sample is raster scanned in two dimensions in the focal plane. Again the finest 50 nm features are resolved.

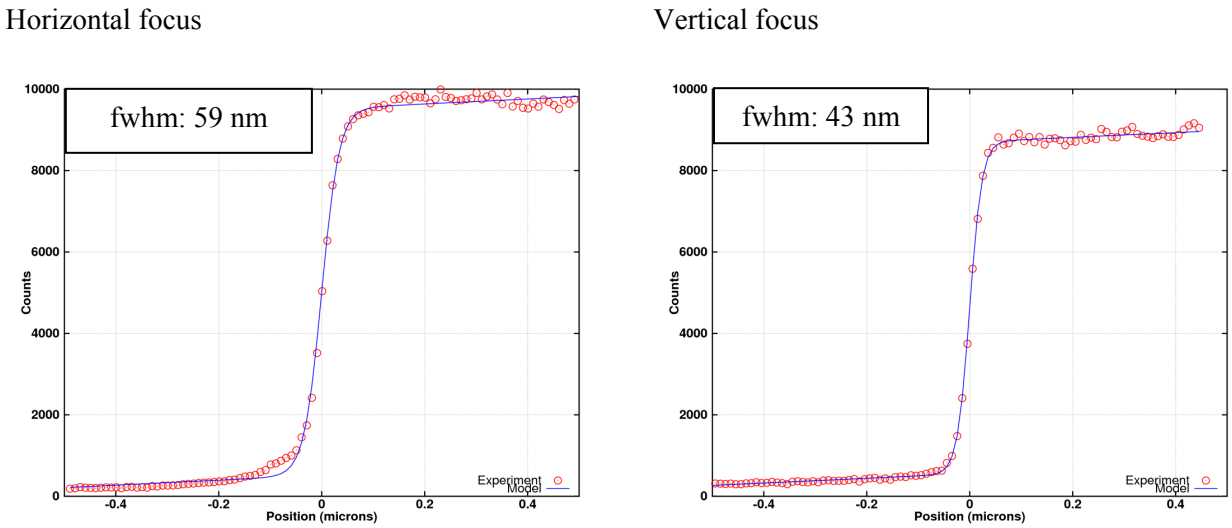


Figure 8: Knife -edge scans (Au L fluorescence detection) across the beam focus at 17 keV

## 4. SUMMARY AND PERSPECTIVES

We have demonstrated that dynamic figuring techniques in the KB configuration can be used for routine focusing with extremely high photon transmission to resolutions < 60nm for hard X-rays. The system presented is now in standard operation at the ID22NI endstation and is used for approximately 75% of experiments in beamline user mode. Attaining such performance is demanding and has required specific expertise in FEA modeling, athermal design methods, multilayer deposition and metrology techniques. We are close to the fracture stresses of the mirror substrates in the current configuration. Further improvements of the acceptance aperture or reduction of the focal length would require the substrate curvature and asphericity to be increased. This would necessitate the use of thinner or more fracture resistant substrates in order to guarantee the system durability. The former might require recourse to deterministic polishing techniques whilst the second would require a rigorous criteria for substrate flaw sizes or the use of other substrate materials (e.g. SiC). An alternative approach would be to prefigure the substrate with a polished spherical radius prior to bending. This was considered for the ID22NI system but the potential reduction in the substrate stresses was modest and could be gained only at expense of a probable reduction in the slope/figure errors of the polished substrate. Nevertheless if a narrower range of grazing angles was required in operation this could be a viable solution if combined with deterministic figure correction of the substrate.

## ACKNOWLEDGEMENTS

The authors thank J. Gregoire, S. Labouré, B. Lantelme, M. Lesourd, G. Malandrino and T. Manning for their expert assistance in the assembly, characterisation and commissioning of the system. The research leading to these results has

received funding from the European Community's Seventh Framework Programme (FP7/2007-2013) under grant agreement n° 226716.

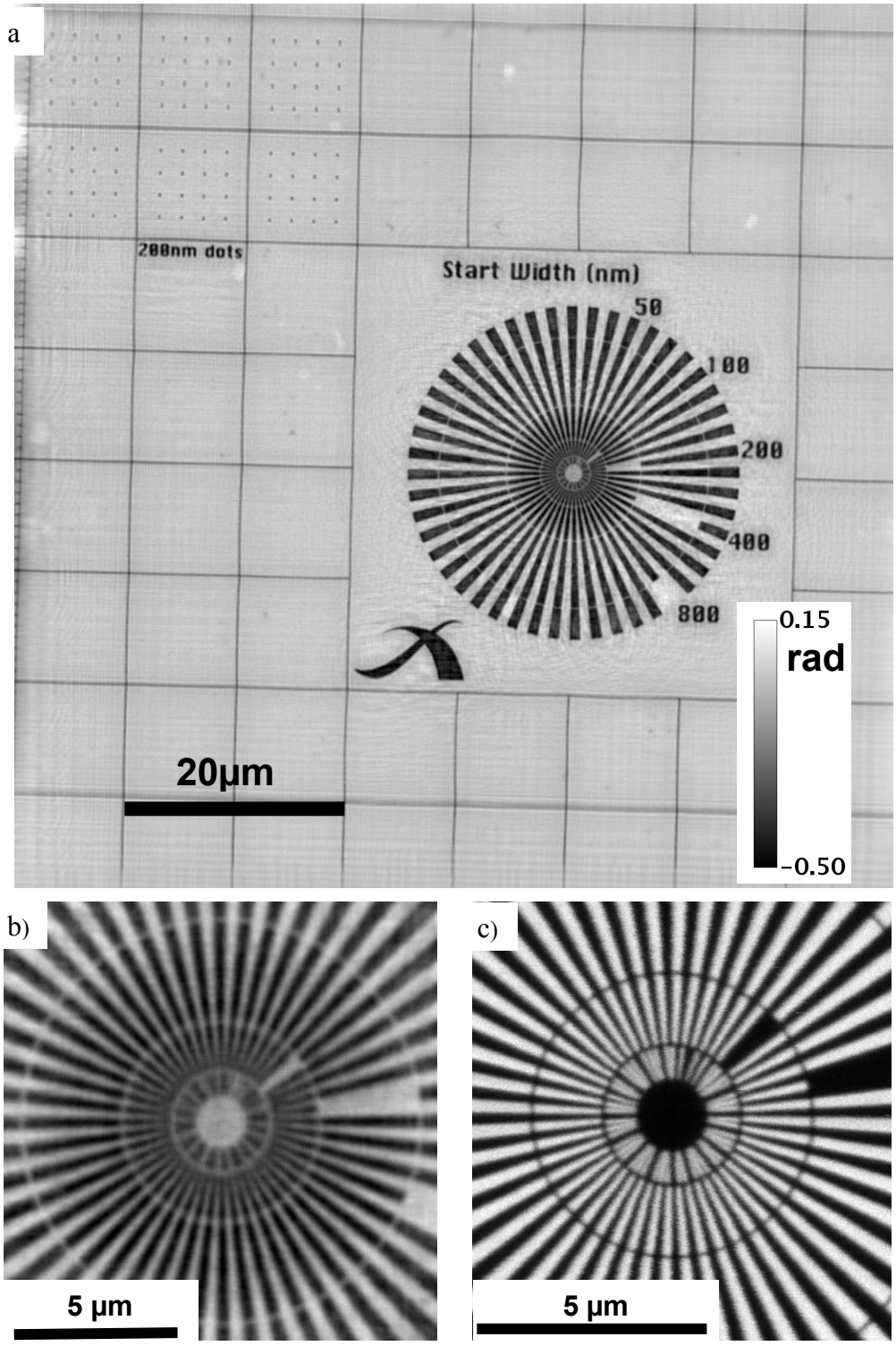


Figure 9: Images of a gold resolution test structure measured at 17.1keV using the ID22NI KB system. a) quantitative phase reconstruction using projection phase-contrast microscopy. b) detail of central region quantitative phase contrast. (same intensity scale) c) Au L X-ray fluorescence map of central zone acquired using raster scanning of sample in focal plane.

## REFERENCES


[1] P. Kirkpatrick and A. V. Baez, "Formation of Optical Images by X-Rays," *J. Opt. Soc. Am.* **38**, 766–773 (1948) [doi:10.1364/JOSA.38.000766].

[2] M. Montel, "X-ray microscopy with catamegonic roof mirrors," in *X-ray Microscopy and Microradiography*, pp. 177–185, Academic Press, New York (1957).

[3] K. Yamauchi, K. Yamamura, H. Mimura, Y. Sano, A. Saito, K. Endo, A. Souvorov, M. Yabashi, K. Tamasaku, et al., "Two-dimensional Submicron Focusing of Hard X-rays by Two Elliptical Mirrors Fabricated by Plasma Chemical Vaporization Machining and Elastic Emission Machining," *Jpn. J. Appl. Phys.* **42**, 7129–7134 (2003) [doi:10.1143/JJAP.42.7129].

[4] W. Liu, G. E. Ice, L. Assoufid, C. Liu, B. Shi, P. Zschack, J. Tischler, J. Qian, R. Khachartryan, et al., "Hard X-ray nano-focusing with Montel mirror optics," *Nuclear Instruments and Methods in Physics Research Section A: Accelerators, Spectrometers, Detectors and Associated Equipment* **649**, 169–171 (2011) [doi:16/j.nima.2010.11.080].

[5] H. Mimura, S. Handa, T. Kimura, H. Yumoto, D. Yamakawa, H. Yokoyama, S. Matsuyama, K. Inagaki, K. Yamamura, et al., "Breaking the 10 nm barrier in hard-X-ray focusing," *Nat Phys* **6**, 122–125 (2010) [doi:10.1038/nphys1457].

[6] M. R. Howells, D. Cambie, R. M. Duarte, S. Irick, A. A. MacDowell, H. A. Padmore, T. R. Renner, S. Rah, and R. Sandler, "Theory and practice of elliptically bent x-ray mirrors," *Opt. Eng.* **39**, 2748 (2000) [doi:10.1117/1.1289879].

[7] P. J. Eng, M. Newville, M. L. Rivers, and S. R. Sutton, "Dynamically figured Kirkpatrick Baez x-ray microfocusing optics," in *Proceedings of SPIE* **3449**, pp. 145–156, SPIE, San Diego, CA, USA (1998) [doi:10.1117/12.330342].

[8] O. Hignette, P. Cloetens, G. Rostaing, P. Bernard, and C. Morawe, "Efficient sub 100 nm focusing of hard x rays," *Rev. Sci. Instrum.* **76**, 063709–5 (2005) [doi:10.1063/1.1928191].

[9] L. Zhang, R. Hustache, O. Hignette, E. Ziegler, and A. Freund, "Design optimization of a flexural hinge-based bender for X-ray optics," *J Synchrotron Rad* **5**, 804–807 (1998) [doi:10.1107/S0909049597015288].

[10] O. Hignette, G. Rostaing, P. Cloetens, A. Rommeveaux, W. Ludwig, and A. K. Freund, "Submicron focusing of hard x rays with reflecting surfaces at the ESRF," in *Proceedings of SPIE* **4499**, pp. 105–116, SPIE, San Diego, CA, USA (2001) [doi:10.1117/12.450227].

[11] O. Hignette, P. Cloetens, C. Morawe, C. Borel, W. Ludwig, P. Bernard, A. Rommeveaux, and S. Bohic, "Nanofocusing at ESRF Using Graded Multilayer Mirrors," *AIP Conf. Proc.* **879**, J.-Y. Choi and S. Rah, Eds., 792–795 (2007) [doi:10.1063/1.2436179].

[12] H. Mimura, H. Yumoto, S. Matsuyama, Y. Sano, K. Yamamura, Y. Mori, M. Yabashi, Y. Nishino, K. Tamasaku, et al., "Efficient focusing of hard x rays to 25 nm by a total reflection mirror," *Appl. Phys. Lett.* **90**, 051903 (2007) [doi:10.1063/1.2436469].

[13] L. Zhang, R. Baker, R. Barrett, P. Cloetens, and Y. Dabin, "Mirror profile optimization for nano-focusing KB mirror," *AIP Conf. Proc.* **1234**, R. Garrett, I. Gentle, K. Nugent, and S. Wilkins, Eds., 801–804 (2010) [doi:10.1063/1.3463335].

[14] B. R. Lawn, *Fracture of brittle solids*, Cambridge University Press (1993).

[15] F. Ebrahimi and L. Kalwani, "Fracture anisotropy in silicon single crystal," *Materials Science and Engineering A* **268**, 116–126 (1999) [doi:16/S0921-5093(99)00077-5].

[16] A. V. Rommeveaux, B. Lantelme, and R. Barrett, "ESRF metrology laboratory: overview of instrumentation, measurement techniques, and data analysis," in *Proceedings of SPIE* **7801**, pp. 780107–780107-11, SPIE, San Diego, California, USA (2010) [doi:10.1117/12.864141].

[17] C. Morawe and J.-C. Peffen, "Thickness control of large area x-ray multilayers," in *Proceedings of SPIE* **7448**, p. 74480H-74480H-10, SPIE, San Diego, CA, USA (2009) [doi:10.1117/12.826121].

[18] O. Hignette, A. K. Freund, and E. Chinchio, "Incoherent x-ray mirror surface metrology," in *Proceedings of SPIE* **3152**, pp. 188–199, SPIE, San Diego, CA, USA (1997) [doi:10.1117/12.295559].

[19] T. Salditt, K. Giewekemeyer, C. Fuhse, S. P. Krüger, R. Tucoulou, and P. Cloetens, "Projection phase contrast microscopy with a hard x-ray nanofocused beam: Defocus and contrast transfer," *Phys. Rev. B* **79**, 184112 (2009) [doi:10.1103/PhysRevB.79.184112].

[20] P. Cloetens, W. Ludwig, J. Baruchel, D. Van Dyck, J. Van Landuyt, J. P. Guigay, and M. Schlenker, "Holotomography: Quantitative phase tomography with micrometer resolution using hard synchrotron radiation x rays," *Appl. Phys. Lett.* **75**, 2912 (1999) [doi:10.1063/1.125225].